GA–A25844

U.S. DCLL TEST BLANKET MODULE DESIGN AND RELEVANCE TO DEMO DESIGN

by
C.P.C. WONG

JUNE 2007

GENERAL ATOMICS

DISCLAIMER

GA–A25844

U.S. DCLL TEST BLANKET MODULE DESIGN AND RELEVANCE TO DEMO DESIGN

by
C.P.C. WONG

This is a preprint of a paper to be presented at the 2nd IAEA Technical Meeting on First Generation of Fusion Power Plants — Design and Technology, Vienna, Austria, June 20–22, 2007 and to be published in the *Proceedings.*

Work supported by
the U.S. Department of Energy
under DE-FC02-04ER54698

GENERAL ATOMICS PROJECT 30200
JUNE 2007

GENERAL ATOMICS

ABSTRACT

In the design of the Test Blanket Module (TBM) for ITER, it is required to provide a design concept that is demonstration power reactor (DEMO) relevant. It should be noted that in the U.S., DEMO is defined to be a good representation of the first generation fusion power reactor. In order to find a relevant DEMO design, a system evaluation was performed with the GA system code, and the physics results were benchmarked to ITER. With the selection of ferritic steel as the structural material, the maximum neutron wall loading is limited to 3 MW/m^2. When designed to a ~2 GW fusion, device an aspect ratio of 2.6 was selected based on this assessment. For the ITER-TBM design, the design guidance is to apply a 2 mm Be layer onto the plasma facing surface. When extrapolated to the DEMO design, the Be layer will not be suitable due to radiation damage. Similarly, a carbon surface will not be suitable due to high physical and chemical erosion rates, radiation damage of the material and potential large retention of tritium. Unfortunately, the remaining commonly proposed material, tungsten (W), could suffer radiation damage from alpha charged particle implantation and experience blistering and the formation of submicron fine structure, which could result in W transport to the plasma core and severely limit the core performance. To resolve this potential impasse, different out-of-the-box options were evaluated. A clear indication was noted that boron or silicon has been used to condition all high performance tokamak experiments. Correspondingly, it is found that in order to maintain a boronized layer on the chamber wall, in-situ boronization will be required. This boronized layer could also protect the W substrate, while retaining low-Z wall characteristics. To support this idea, an invention on the use of boron-infiltrated W-mesh surface is proposed to withstand ELMs and disruptions while retaining the capability of transmitting high grade heat for power conversion. Initial development and identified requirements for this BW-mesh concept will be reported.

1. INTRODUCTION

In the selection of tritium breeding blanket concepts to be tested in ITER, the world community is focusing on the use of ferritic steel as the suitable structural material for DEMO and beyond. Technical consensus has also been reached that the maximum allowable neutron wall loading (Γn) located at the outboard midplane of a tokamak is around 3 MW/m^2 [1]. It becomes prudent to search for a reasonable DEMO design for the US-TBM program. For this paper, only modest extrapolation from ITER baseline physics is applied. The DEMO selected in 2004 after the U.S. rejoined the ITER project has an aspect ratio (A) of 2.6. Further details of the systems code results will be presented. For the second part of this paper, we are addressing the selection of the chamber wall material for DEMO. For the ITER-Test Blanket Module (TBM) design, the design guidance from ITER is to apply a 2 mm Be-layer onto the plasma facing surface. But Be could suffer radiation-induced swelling and corresponding loss of ductility [2], which most likely will not be acceptable for DEMO. Correspondingly, the most commonly selected materials like C and W will also suffer radiation damage at high neutron and helium charged particle fluence, respectively [3-6]. This leads to the consideration of alternative approaches for the first wall material. Accordingly, a boron-loaded W-mesh approach, which could be suitable for DEMO application, is presented in this paper.

2. DEMO

For the ITER TBM design, the proposed blanket concepts have to be relevant to the DEMO design. For the definition of the DEMO, a simple systems code was used for the assessment [7]. The design goal is to find a DEMO design with maximum outboard midplane neutron wall loading of 3 MW/m^2. As input physics parameters, we initiated the assessment using impurities concentrations and plasma temperature, density profiles and other parameters specified by ITER as shown in Case 1 of Table I. A key evaluation factor is also the inboard compressive stress at the inboard side of the TF coil. For benchmarking calculations, at an equivalent coil current density of 6.5 MA/m^2 the ITER design compressive loading stress limit is used, which corresponds to about 85% of the value used by the ARIES-AT design [8]. The assumed thermal power conversion efficiency is 40%. These results were generated in 2004 after the U.S. rejoined the ITER project.

Table I
SIX Cases for the Assessment of a Set of Parameters for DEMO for ITER-TBM

Characterization	1 ITER	2 Simulated ITER	3 Higher β_N	4 Lower A	5 Increase n_e/n_{GW}	6 A = 2.6
R_0, m	6.2	6.2	6.2	6.02	5.91	5.8
A	3.1	3.1	3.1	2.8	2.7	2.6
β_N	2	1.8	2.4	2.49	2.53	3.19
Height, m		7.4	7.4	8.03	8.21	8.4
Pfusion, MW	500	475	757	2089	2103	2116
Max. Γ_N, MW/m^2	0.78	0.702	1.12	3.007	3.045	3.082
P_e-net, MWe	NA	315	577	1677	1649	1690
Reactor ave. first wall ϕ, MW/m^2	0.3	0.123	0.16	0.385	0.408	0.396
n_e/n_{GW}	0.85	0.84	0.84	0.84	1	1
Inboard coil buckling force,* MPa		1271	1271	1730	1361	1003
B_0, T	5.3	5.28	5.28	6.34	5.7	5.02
β_t,%	2.5	2.5	3.3	4.1	4.5	6.1
β_p	0.72	0.65	0.87	0.765	0.731	0.862
κ	1.85	1.85	1.85	1.866	1.874	1.886
Z_{eff}	1.72	1.6	1.624	1.647	1.629	1.638
I_p, MA	15	15	15	23	22.76	21.88
ndt, 10^{20}	1.13	0.84	0.81	1.02	1.2	1.09
T_{max}/T_{ave}, keV		21/8	29.5/11.2	41.9/15.9	31.5/11.9	36.2/13.7
H98y2	1.00	0.966	1.17	1.00	0.893	1.05

*The limit from ARIES-AT is 1206 MPa

Table I shows Case 2 as a simulation of the ITER design and 4 other cases modified from the ITER design:

1. ITER design
2. Simulated ITER design
3. Increase the fraction of β_N from 40% to 53% of the optimum β_N based on MHD stability calculation [9]
4. Decrease A from 3.1 to 2.8
5. Decrease A to 2.7 and increase Greenwald density limit from 0.8 to 1, which is an input parameter for this systems calculation
6. After some iterations, we selected Case 6 (A=2.6) for our DEMO design. Case 6 consists of favorable design parameters and satisfies the inboard coil buckling loads lower than that of ITER.

It should be noted that these results were obtained using a relatively simple systems code to generate a set of DEMO parameters. In the future, a much more complete assessment should be performed to determine the more optimized US-DEMO design.

3. SYSTEM CODE CALCULATION AND RESULTS

Subsequent to 2004, we continued to improve the GA systems design code. The improvement includes better parametric representation of the plasma elongation and alpha impurity content. To match the ITER physics performance [10], the β_N value of 2 is used, which corresponds to 42% of the maximum achieved by stability calculations [9]. A comparison with the ITER reference point design is given in Table II. The results are well matched.

Table II
Comparison of ITER Design and GA System-Code Generated Parameters

	ITER	GA-Code		ITER	GA-Code
Total fusion power, MW	500	529	Triangularity	0.48	0.48
Max. Γ_n, MW/m^2	0.78	0.78	B_0, T	5.3	5.3
R_0, m	6.2	6.2	q at 95% flux surface	3	3.
a, m	2.0	2	Plasma vol., m^3	831	848
A	3.1	3.1	Plasma area, m^2	683	742
τ_{He}/τ_E	5	5	Input Power total, MW	151	102
n shape factor	Flat	0.25	Ave. T_i, keV	8.9	12.8
T shape factor	Peak	1.5	n_e/n_{GW}	0.85	0.75
β_N	2	2	H-factor-98 (y,2)	1	1.07
β_t,%	2.5	3	Z_{eff}	1.72	1.89
I_p, MA	15	15.6	He fraction	0.032	0.03
κ	1.85	1.85	τ_E	3.4	2.02

With the use of ITER inboard TF coil design (inboard conductor radius of 3.5 m, and a bore of 2.05 m), different design parameters were generated as a function of A with the same central TF coil current density of 6.5 MA/m^2. Results are shown in Case 1 of Table III. Due to the higher performance of β_t at lower A, the corresponding fusion power is much higher at lower A. Fusion power output varies from 15 GW at A=1.8 to 5.5 MW at A=6. But for A < 2.5, the $n_e/n_{GW} \geq 1.1$ which is not desirable.

For a device like a Component Testing Facility (CTF), the machine can be designed to a maximum Γ_n = 1 MW/m^2 with a change in central column current density as shown in Case 2 of Table III, again using ITER inboard design geometry. The physics parameters for Case 2 are reasonable as represented by n_e/n_{GW} less than 1 for A > 2.5. But for A = 5 and 6, with fusion power > 300 MW, the compressive loads will be respectively 2 to 3 times higher than the ITER case. In general, this study shows the difficulty of designing a CTF with an inboard design similar to ITER, which is a good representation of an SC coil design. The power output will need to be high (> 400 MW) while satisfying the inboard buckling force loads.

Table III
Performance Versus Aspect Ratio A for ITER-Like SC Device and for MAXIMUM Γ_N = 1 MW/m^2 (Case 2) at the Outboard Midplane

		Case 1 Design to ITER Physics, $\beta_N = 2$ @ A = 3.1 Compressive Buckling Load @ 1029 MPa, J_c = 6.5 MW/m^2					Case 2 SC Coil Design to Maximum Γ_n = 1 MW/m^2 $\beta_N = 2.88$ @ A = 3.1				
Aspect Ratio (A)	R_0 (m)	β_N	Max. Γ_n (MW/m^2)	Fusion Power (MW)	$\beta_t B_T^2$	n_e/n_{GW}	β_N	Equivalent[a] J_c (MA/m^2)	Compressive Load	Fusion Power (MW)	n_e/n_{GW}
1.8	9.5	2.83	5	15200	1.3	1.8	4.09	3.0	222	3201	1.24
2	8.4	2.66	4	8618	1.3	1.56	3.84	3.2	249	2264	1.1
2.5	7	2.3	1.9	2209	1.1	1.1	3.33	3.8	352	1142	0.91
3	6.3	2.05	0.9	663	0.9	0.8	2.85	4.7	526	748	0.82
3.5	5.9	1.84	0.4	229	0.7	0.6	2.66	5.6	761	532	0.76
4	5.6	1.67	0.2	91	0.5	0.5	2.42	6.6	1065	405	0.72
5	5.3	1.43	0.07	19	0.3	0.3	2.07	8.9	1911	269	0.66
6	5	1.26	0.03	5.5	0.2	0.2	1.82	11	3164	208	0.60

[a]Equivalent = current density averaged over the coil geometric area.

4. TOKAMAK CHAMBER WALL MATERIAL

ITER has selected Be as the first wall material, and C and W as the divertor surface materials. These are commonly selected materials for experimental pulse operation tokamak devices. B is also commonly used as the material for wall conditioning for both metallic and graphite wall experimental non-DT fuel devices, and Si has also been used for the same purpose. For DEMO, when the selection of chamber wall material is considered, the additional impacts from steady state operation and radiation damage from neutrons and charged particles will have to be taken into consideration. The measured erosion rate for metallic materials of interest is shown in Fig. 1 for a heat flux of ~0.7 MW/m^2 in DIII-D [11]. As shown, the measured erosion rate is lower than the modeled sputtering yield. The corresponding measured graphite wall erosion rate is about 4 nm/s under similar heat flux.

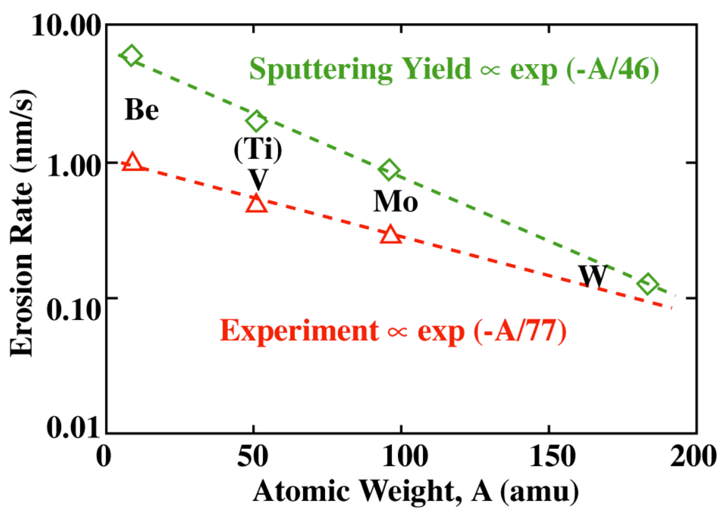

Fig. 1. Erosion rate as a function of atomic weight of chamber surface material [11]. (The divertor heat flux is 0.7 MW/m^2 and corresponding measured erosion rate for DIII-D divertor graphite tile is 4 nm/s.)

As shown, Be has an erosion rate at the divertor only about one-fourth that of graphite, which means that the erosion rate for both C and Be would be too high when extrapolated to higher heat flux of 2–10 MW/m^2 and for steady state operation. Furthermore, both C and Be will also suffer radiation damage in the form of swelling and have a corresponding degradation of mechanical properties, which would make them unsuitable for use in DEMO. Figure 1 shows that W has the lowest erosion rate and is the preferred chamber surface material for DEMO. However, laboratory experiments indicate internal damage on powder metal (PM)W surface from He ion irradiation from room temperature to 873 K for He^+ fluence up to 2.5x10^{21} even at energy of <1 keV [8]. At higher temperature of 1200 K and with lower energy He^+ at 11.3 eV, results showed blackening of the W-surface with formation of submicron fine structure [9], which is also confirmed by results from PISCES-B with He^+ energy of 25 eV

[10]. Even though the formation mechanism of the submicron fine structure is not understood, these are not encouraging indications for the application of W for DEMO. With the goal of resolving some of the fundamental problems on the selection of chamber surface material, unconventional approaches were evaluated by the fusion community, including liquid metal surface for the chamber wall and divertor. More recently, the boron-infiltrated W-mesh (BW-mesh) concept was conceived.

4.1. BW-MESH CONCEPT AND OBSERVATIONS

The basic idea of the BW-mesh concept is the following:

A W-mesh as shown in Fig. 2 can be infiltrated with boron, with the goal of filling in all the pores and having a coating of B covering the W surface facing the plasma. Methods of loading/infiltration are being evaluated, which can include methods like high temperature diffusion, physical infiltration at low temperature, chemical vapor infiltration or plasma spray.

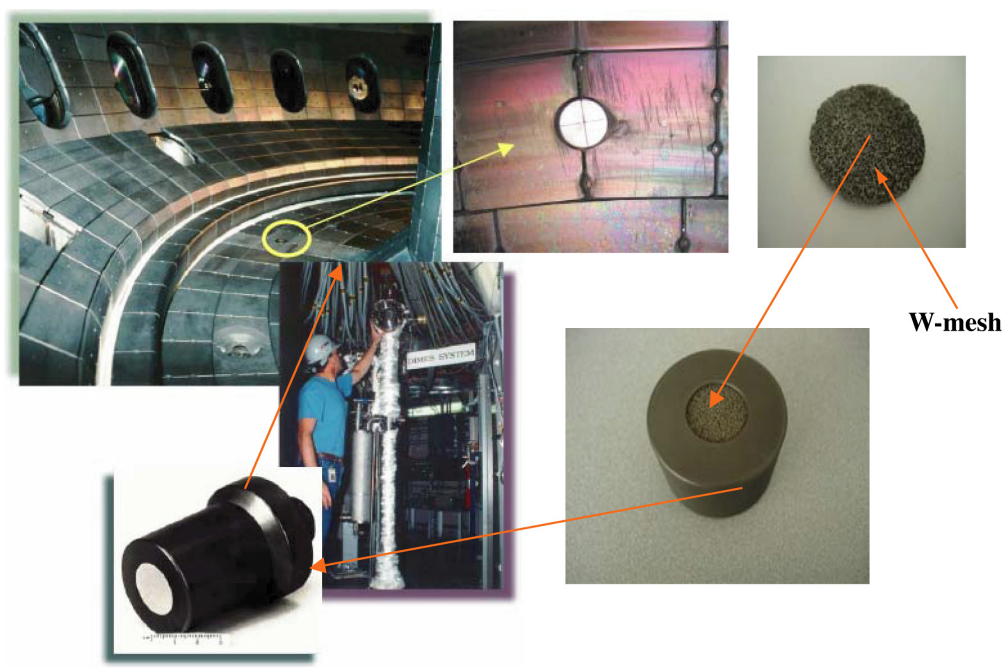

Fig. 2. DiMES system in DIII-D and a W-mesh sample.

The key for the concept is to only have B-surface exposed to the plasma, thus reducing any negative impact to the plasma burn. The W-mesh is to trap enough B to withstand the energy deposited from occasional ELMs and disruptions. Since each disruption would remove about 100 μm of B, a net B thickness of 1 mm could take a few disruptions. For a BW-mesh thickness of about 2 mm, the W-mesh open porosity should be about 50%. Considering the small mean-free path of the helium-charged particles from the plasma, a thin coating of B should protect the W from radiation damage caused by He ions. Since the goal for this BW-mesh concept is for steady state operation, a means of in-situ boronization during the plasma discharge is needed. The above characteristics are design goals that could be demonstrated in existing tokamak devices. The BW-mesh thickness of 2 mm is selected for the maintenance of adequate heat transfer through the layer to the substrate structure and to the active coolant, while relying on the high thermal conductivity of W-metal. An equivalent thermal conductivity of the BW-mesh of 20 W/m.k is the design goal.

Since B will experience physical erosion similar to carbon, the in-situ boronization needs to satisfy three design functions: to replenish the eroded B during normal operation, to replenish the B after a disruption and to make sure that the W-mesh is not exposed. Since most of the boron deposition would be localized, this could mean the necessary strategic positioning of B injectors. Similar to carbon, tritium will also be picked up by the boron surface, but as shown in Fig. 3, nearly all the absorbed tritium could be released at ~ 400°C. For DEMO design, since the maximum ferritic steel first wall structure would be designed to operate at ~500-550°C, the surface temperature of the BW-mesh should be high enough for continuous release of trapped tritium. Boron is actually a material very familiar to tokamak operation, since it is one of the most commonly use materials for chamber wall conditioning and has been used in DIII-D, NSTX, TEXTOR, JT-60U, C-Mod, ASDEX-Upgrade, JFT-2M, LHD, and HT-7, for example, where different compounds of B have been used. Similarly, many attempts on in-situ boronization have been tried in various devices including DIII-D, NSTX, TEXTOR, TdeV, and PBX-M. Perfect in-situ B-coating to all surfaces has not yet been shown, possibly due to inadequate experimental time and the limited number of B injection locations.

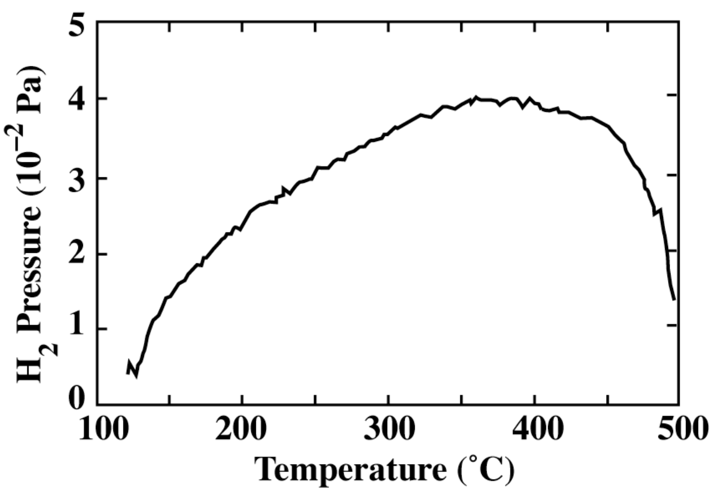

Fig. 3. Hydrogen pressure as a function of temperature. All the implanted hydrogen atoms in a boron film are released below 400°C [12].

For the successful application of this BW-mesh concept, in addition to in-situ boronization, other critical issues will surface. As an example, one of the needed technology developments will be the attachment of the BW-mesh layer to the substrate material like ferritic steel while maintaining adequate heat transfer. Other technology areas such as the tokamak vacuum system and tritium extraction system will also be impacted. Other issues will also be identified and uncovered, and will need to be resolved in the future as the BW-mesh concept gets further developed.

4.2. PROPOSED BW-MESH DEVELOPMENT IN DIII-D

For the development of the BW-mesh concept, the following plan using the DiMES apparatus shown in Fig. 2 has been proposed:

1. High purity B-dust will be introduced with DiMES at the lower divertor of DIII-D and its transport in the plasma chamber will be studied, including the deposition at the midplane location with removable material samples using the midplane material evaluation system (MiMES).
2. A B-infiltrated BW-mesh sample will be exposed to routine plasma operation, ELMs and disruptions in DIII-D.
3. Further experiments on in-situ boronization.

We are now at the stage of investigating different methods of infiltrating different types of W-mesh with B.

5. CONCLUSIONS

Using the GA system code and the same inboard design geometry and dimension as ITER, and accounting for the technology constraints of the inboard superconducting coil design and the selected neutron wall loading, the following observations on fusion power as a function of A can be made. For higher fusion power, lower A is preferred but constrained by physics and inboard coil stress. To select a set of DEMO parameters with a maximum neutron wall loading of 3 MW/m^2, this study found that a machine with A = 2.6 is reasonable. For a superconducting coil testing device like CTF with fusion power ~400 MW, the preferred A is large at around 4. Results are sensitive to the achievable physics performance of the machine but still subject to the technology limits from the TF coil design and the acceptable maximum neutron wall loading.

For the selection of chamber wall material for DEMO, commonly used materials like C, Be and W would likely not be suitable due to high physical erosion rates and/or radiation damage from neutrons and/or helium ions. The invention of the BW-mesh concept may help alleviate many of the concerns. The key is for the replenishment of the B surface, but this will require the successful demonstration of in-situ boronization and the addition of boron as another consumable material for the steady state operation DEMO. This BW-mesh concept is at a very early stage of development, but the initial step has been taken in the fabrication of the BW-mesh sample to be tested in DIII-D.

REFERENCES

[1] GIANCARLI, L., et al., "Test Blanket Modules in ITER: an overview on proposed designs and required DEMO-relevant materials," Fusion Reactor Materials (Proc. 12th Int. Conf., Santa Barbara, 2005) to be published.

[2] GELLES, D.S., et al., "Radiation Effects in Beryllium Used for Plasma Protection," J. Nucl. Mater. **212-215** (1994) 29.

[3] BARABASH, V., et al., "Material/Plasma Surface Interaction Issue following Neutron Damage," J. Nucl. Mater. **313-316** (2003) 42.

[4] YOSHIDA, N., Plasma-Facing Materials and Components for Fusion Applications (Proc. 11th Intl. Wkshp., Greifswald, 2006) to be published.

[5] YOSHIDA, N., Diagnostics (Proc. IEA 12th ITPA Mtg. Princeton, 2007) to be published.

[6] BALDWIN, M.J., US PFC Meeting, ANL, June 4-7, 2007.

[7] WONG, C.P.C., et al., "Toroidal Reactor Designs as a Function of Aspect Ratio and Elongation," Nucl. Fusion **42**(5) (2002) 547.

[8] MILLER, R.L., and the ARIES Team, "System Context of the ARIES-AT Conceptual Fusion Power Plant," The Technology of Fusion Energy 2000 (Proc. 14th Topl. Mtg., Park City, 2000) Fusion Technol. **439-443,** Number 2, part 2 (2001) 39.

[9] LIN-LIU, Y.R., "Optimum Equilibria for High Performance, Steady State Tokamaks," Nucl. Fusion **44**(4) (2004) 548.

[10] "ITER Technical Basis," ITER Report G A0 FDR 1 00-07-13 R1.0.

[11] WONG, C.P.C., et al., "Divertor Material Evaluation System (DiMES)," J. Nucl. Mater. **258-263** (1998) 433.

[12] NODA, N., "Boronization in Future Devices-Protecting Layer Against Tritium and Energetic Neutrals," J. Nucl. Mater. **266-269** (1999) 234.

ACKNOWLEDGMENT

This work supported by the U.S. Department of Energy under DE-FC02-04ER54698.